*33rd EPS Conference on Plasma Phys. Rome, 19 - 23 June 2006 ECA Vol.**30I**, D-5.018 (2006)*

Self-consistent 2D simulations of plasma deposition in tile gaps

R. Dejarnac[a] and J. P. Gunn[b]

[a]*Association EURATOM-IPP.CR, Prague, Czech Republic*

[b]*Association EURATOM-CEA, Centre de Cadarache, 13108 Saint Paul Lez Durance, France*

1. Introduction

In order to withstand thermomechanical stress in ITER's divertor, its armour will be castellated [1]. Carbon layers and tritium will accumulate inside the gaps that separate the tiles. Experimental studies [2] already show significant deposited layers in the gaps. We present here a two-dimensional numerical study of plasma deposition inside the tile gaps using a standard particle-in-cell (PIC) technique (section 2). The plasma deposition with respect to the depth and the width of the gap for different inclinations of the magnetic field lines are performed (section 3). Particle flow asymmetries occurring inside the gap are of particular interest. A summary of the results and the conclusions are presented in section 4.

2. Tile gap modeling

The numerical tool we have developped for this study is a three velocity – two-dimensional kinetic code based on PIC technique [3]. The code is based on the resolution of the equations of motion and the integration of Poisson's equation to obtain the self-consistent electric field that accelerates the particles. The novelty of the code is its ability to inject arbitrary velocity distribution functions. For the ions, we use a non-Maxwellian distribution given by a one-dimensional quasineutral kinetic calculation of the scrape-off layer [4, 5] that satisfies the kinetic Bohm criterion at the sheath entrance. The case considered here is a fully ionized magnetized plasma with one species of singly charged ions incident on a completely absorbing, conducting wall. The uniform magnetic field $\boldsymbol{B}$ can have an arbitrary orientation. A magnetic sheath [6, 7] can thus develop along the surface in the range of 4 r_L, where r_L is the Larmor radius. This has been taken into consideration by assuring a minimum distance of *10* r_L in between the tiles top and the plasma boundary in order to have no perturbation of the bulk plasma. The length of the tile tops is also taken large enough to avoid perturbations generated by the gap itself due to the periodicity of the system. We verify that the solution at the boundaries is identical to the semi-infinite 1D solution. In our simulations, we set n_e=3.5x10^{18} m^{-3}, T_e=25 eV, B= 5 T, to model a moderate flux zone with a partially magnetized sheath. These conditions are favorable for the growth of thick carbon deposits inside tile gaps in the Tore Supra tokamak.

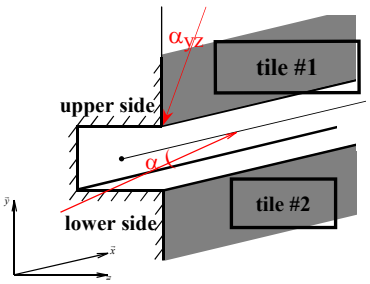

Figure 1: Scheme of the simulation domain in Cartesian coordinates.

We simulate two types of gaps according to their orientations with the magnetic field lines: gaps perpendicular to ***B*** (poloidal gaps) and gaps parallel to ***B*** (toroidal gaps). In the following, we will only use the incident angle α of the field lines with the surface and the gap orientation to describe the geometry. In ITER, the vertical target will consist of castellated *10x10mm* tiles with a gap width of *0.5mm*. The incidence of the field lines should be at most *5°*. We have investigated two angles, α = *5°* and α = *20°* (like in [2]) for both poloidal and toroidal gaps, as well as two different gap widths, l_{gap}= *0.5mm* and l_{gap} = *1mm*.

3. Results and discussion

For better understanding, we use the terms *vertical* and *horizontal* relatively to the *y*- and *z*- directions, respectively (see Fig.1). With the same convention, the two sides of the gap are named *upper side* and *lower side*.

3.1. Poloidal gaps

The electric potential distribution in the simulation region shows a strong positive peak inside the gap (Fig.2a). This structure is due to the different degree of magnetization of ions and electrons. Electrons remained tied to the ***B*** lines, but ions can move freely in the horizontal direction due to their Larmor gyration and the polarization drift [7]. This leads to strong positive charge separation. Fig.3a shows the vertical ion flux falling onto the two sides of the gap along the horizontal axis. This flux is normalized to the theoretical unperturbed flux that impinges on the tile far from the gap. Around 70% of the incident ion flux flows downward on the wetted side of the gap. Some flux (only <1%) is collected on the magnetically shadowed upper side due to parallel flow reversal of the ions that just graze the edge of the

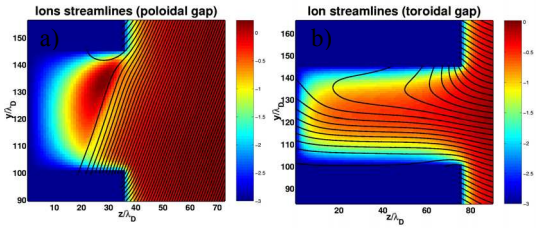

Figure 2: Ion streamlines in the case of poloidal (a) and toroidal (b) gaps plotted over the electric potential normalized to kT_e/e for the reference case, i.e, an angle of 20° and a gap width of 1mm.

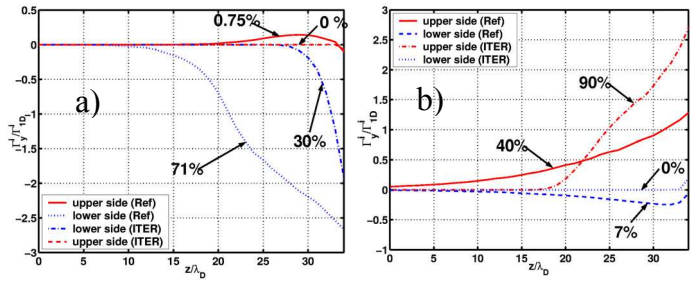

Figure 3: Vertical ion flux falling on the sides of the gap for poloidal (a) and toroidal (b) cases normalized to the non-perturbed influx flowing onto tile surface for the case (20°, 1mm) and (5°, 0.5mm). The percentages correspond to the total incident current normalized by the sheath edge current density integrated across the gap entrance.

upper tile and get reflected by the positive potential inside the gap. The missing incident flux is expelled from the gap by the charge separation field; they continue along field lines to be collected on the leading edge of the lower tile (Fig. 2a). Fig.4a shows the ion flux perpendicular to the tiles normalized by the theoretical 1D influx. The flux at the upper part of tile#1 and at the lower part of tile#2 is constant and corresponds to the influx injected from the plasma side. We observe in the gap interval a decrease of the horizontal flux that is compensated by an increase of the vertical flux in this area. Indeed, we observe a significant increase of the horizontal particle flux deposited on the leading edge of tile#2. This confirms that a non-negligible fraction of the ions flowing into the gap in the parallel direction is expelled by the charge separation potential to be deposited on the top of tile #2 within *1mm*.

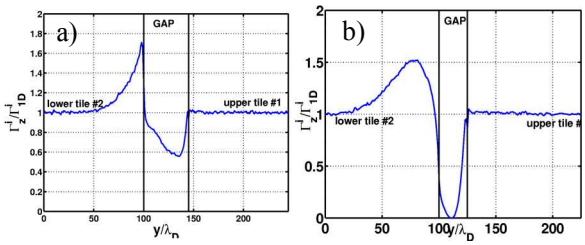

Figure 4: Horizontal ion flux normalized to the non-perturbed influx flowing onto tile surface along the vertical coordinate at gap entrance for a poloidal gap for a) reference case (20°, 1mm) and b) ITER (5°, 0.5mm).

In the ITER case (l_{gap}=*0.5mm*, α=*5°*), due to such a small incident angle, only few particles enter the gap, therefore the particle flux deposited on the two sides on the gap is strongly reduced (Fig.3a). No particles are collected by the upper side while 30% of the incident influx is found on the lower side (with a corresponding power load of 1-2 MW/m^2 within 0.15mm). Decreasing the angle of incidence thus leads to an increase of the flux expulsion onto the lower tile#2 (Fig.4b). Simulations for H^+ ions give a total power flux of 0.8 MW/m^2 on the unperturbed tile#1 and a peak value of 1.2 MW/m^2 on the lower tile#2 within 1.5mm where the tile wetted by the deflected flux.

3.2. Toroidal gaps

In the case of toroidal gaps (Fig.2b), there is a strong asymmetry in particle trajectories caused by the ***ExB*** drift in the magnetized sheath; at the tile surfaces this drift is directed upwards along the y- axis. Inside the gap, the ***ExB*** drift tends to sweep ions preferentially onto the upper surface. There, the drift can even cancel the incoming parallel flow, leading to a purely vertical flow onto the upper side of the gap. Fig.3b shows that 40% of the influx is collected on the upper side of the gap and 7% on the lower side. The gap was not deep enough for the reference case of 20°, so a significant amount was also collected on the bottom of the gap (45%). Presumably this flux would go to the upper side if we had simulated a deeper gap. The missing flux (8%) is not expelled as in the case of poloidal gaps, but is lost before entry due to strong focusing of the electric field on the corner of tile #2 (Fig.5a).

In the ITER case (l_{gap}=*0.5mm*, α=*5°*), we observe the same strong asymmetric deposition with no particles collected on the lower side (see Fig.3b). Roughly the same amount of influx is collected inside the gap (90% in this case compared to 92% in the reference case), but it is more concentrated near the gap entrance. In fact, practically no ions penetrate to the floor of the gap. This is due to the fact that the ***ExB*** drift dominates the horizontal projection of the parallel inflow for nearly grazing ***B*** angles. The power flux inside the gap is of the same order than poloidal gaps (1-2 MW/m^2) but is spread on a wider area (0.35mm).

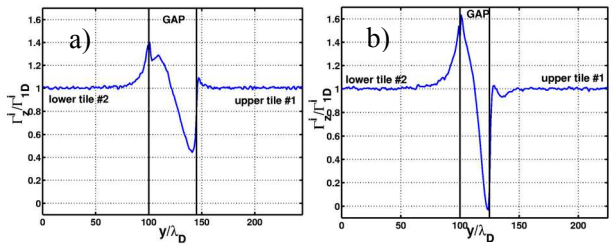

Figure 5: Horizontal ion flux normalized to the non-perturbed influx flowing onto tile surface along the vertical coordinate at the gap entrance for a toroidal gap for a) reference case (20°. 1mm) and b) ITER (5°. 0.5mm).

4. Summary and conclusions

Plasma deposition is asymmetric in both poloidal and toroidal castellated tile gaps. Particle collection is a function of the gap dimension and the incidence of magnetic field lines. Strong electric fields developed along the sides of the gap govern the trajectories with the orientation of the magnetic field due to ***ExB*** drifts. In case of small poloidal gaps with grazing magnetic field lines, most of the incident ion flux is diverted over the entrance of the gap by the charge separation field and collected over *1mm* of the leading edge of the downstream tile. This will lead to significantly enhanced local power loading, so these findings should be taken into account in thermomechanical modeling of the tiles. In the case of toroidal gaps, practically all the flux that enters will impinge on the side favored by the ***ExB*** drift. This finding is consistent with the observation that carbon layers form preferentially on the high field side of toroidal gaps on the toroidal limiter in Tore Supra [8] (***B*** is oriented in the negative toroidal direction). A small amount (10%) of the influx is focused onto the leading corner of the tile face. This result might be different in the case of beveled corners, and for misalignments of the gap with respect to the magnetic field; we will investigate these issues in the future.

Acknowledgements

This work has been done under the Euratom fellowship Contract No 012801 (FU6).

References

[1] W. Daener et al., Fusion Eng. Des. **61&62**, 61 (2002).
[2] A. Litnovsky et al., J. Nucl. Mater. **337-339**, 917-921 (2005).
[3] C.K. Birdsall and A.B. Langdon, *Plasma Physics via Computer Simulation* (1985).
[4] V. Fuchs et al., 32nd EPS Plasma Physics Conference, Tarragona 2005.
[5] J. P. Gunn, J. Nucl. Mater. **337-339**, 310 (2005).
[6] R. Chodura, Phys. Fluids **25**, 1628 (1982).
[7] J. P. Gunn, Phys. Plasmas **4,** 4435(1997).
[8] C. Brosset, private communication (2006).